Journal of the Korean Physical Society, Vol. 44, No. 2, February 2004, pp. 369∼375

Structural Aspects of the Charge Disproportionation Transition in $La_xSr_{1-x}FeO_{3-y}$ (x = 1/10, 1/3, and 1/2)

Sung Hyun YOON*
Department of Physics, Kunsan National University, Kunsan 573-701

Chul Sung KIM
Department of Physics, Kookmin University, Seoul 136-702

(Received 29 September 2003)

The aspects of the charge disproportionation transition for polycrystalline $La_xSr_{1-x}FeO_{3-y}$(x = 1/2, 1/3, and 1/10) near the transition temperature are investigated using Mössbauerspectroscopy in relevance with their chemical and crystallographic data.

As the lanthanum content x is increased, both the rhombohrdral lattice constant a_R and the edge angle α_R increase, resulting in a slight increase in the tolerance factor t. For x = 1/3, a first-order-like transition between the low-temperature antiferromagnetic mixed-valence state and the high-temperature paramagnetic average-valence state takes place in the temperature range between 175 K and 200 K. With an increase in x from 1/3 to 1/2, this transition becomes blurred by the weakened p-d hybridization due to the slight decrease in the bond angle ($\angle$Fe-O-Fe) from 180° with its transition temperature effectively unchanged. For the case of x = 1/10, the electron delocalization takes place at considerably low temperature, and $La_xSr_{1-x}FeO_{3-y}$is paramagnetic in the temperature region examined. This comes from a reduction of electron transfer energy due to contractions in the bond lengths.

PACS numbers: 76.80.+y
Keywords: Mossbauer spectroscopy, Perovskite, Charge disproportionation

I. INTRODUCTION

In some respects, the carrier-doped iron perovskite $La_xSr_{1-x}FeO_{3-y}$(LSFO) exhibits several peculiar properties different from those of hole-doped manganites $La_{1-x}A_xMnO_{3-y}$(A = Ca or Sr). Hole-doped manganites show remarkably varied properties that depend on compositions, temperatures, and the species of substituted atom [1]. A typical example among them is the so-called metal-insulator transition, and the transition temperature happens to coincide with the magnetic transition temperature. On the other hand, the iron perovskite is free from the Jahn-Teller distortion, despite its $Fe^{4+}(d^4)$ nature, and in some cases, it shows no metal-insulator transition. This is an intriguing behavior in view of the facts that iron perovskites are the same charge-transfer-type insulator as manganites [2] and that both perovskites contain atoms with similar electronic structures (Fe^{4+} and Mn^{3+}). It is now believed that this difference originates from existence, or non-existence, of the charge disproportionation(CD) transition. Unlike in the case of manganites, hole-doped iron perovskites avoid any structural instabilities like the Jahn-Teller distortion by generating CD state.

This unique CD transition was first proposed two decades ago based upon Mössbauerspectroscopic comparison of $SrFeO_3$ and $CaFeO_3$. A Mössbauerstudy of $CaFeO_3$ [3] revealed a pair of hyperfine sextets of equal intensity at 4.2 K with the Mössbauerparameters H_{hf} = 41.6 T, δ_{is} = 0.34 mm/s and H_{hf} = 27.9 T, δ_{is} = 0.00 mm/s. On heating, the two sextets merged into two singlets of equal intensity at 116 K, meaning that Néeltemperature had been reached. Further heating converted the spectrum into a singlet at 300 K. The former transition at 116 K was interpreted as a change from an antiferromagnetically ordered mixed valence Fe^{3+}/Fe^{5+} state to a paramagnetic mixed valence state. The latter one at 300 K is the so-called metal-insulator transition at which the paramagnetic insulating mixed valence Fe^{3+}/Fe^{5+} state is converted to a paramagnetic metallic average valence Fe^{4+} state as indicated in the charge disproportionation

$$2Fe^{4+} \rightleftharpoons Fe^{3+} + Fe^{5+}. \quad (1)$$

This charge disproportionation, however, does not take place in $SrFeO_3$, which is structurally related to $CaFeO_3$. It is a metallic conductor with a Néeltemperature of 134

*E-mail: shyoon@kunsan.ac.kr

K and remains cubic down to 4.2 K, showing a single magnetic sextet with $H_{\rm hf} = 33.1$ T and $\delta_{\rm is} = 0.146$ mm/s [4]. The absence of Jahn-Teller distortion in this high spin $3d^6$ state was explained by using the high electrical conductivity where the e_g^* orbitals are broadened into an itinerant electron conduction band.

Earlier Mössbauerstudies of LSFO were performed by Shimony and Knudsen [5]; they merely observed characteristic Fe^{4+} spectral lines at high values of x and a Fe^{3+}/Fe^{4+} mixed state at intermediate x. However, the Mössbauerintensity ratio was far from that expected from the formula $La_xSr_{1-x}Fe_x^{3+}Fe_{1-x}^{4+}O_3$. Takano *et al.* [6] found that the Fe ions could take indiscrete charge states between Fe^{3+} and Fe^{5+}, depending on the composition. Subsequently, he suggested the existence of a non-integral oxidation state of iron in this material following a disproportionation of the type

$$2Fe^{4+} \rightleftharpoons Fe^{4+\lambda} + Fe^{4-\lambda} \quad (2)$$

and modified the chemical formula as

$$La_xSr_{1-x}Fe^{(3+\delta)+}_{(1+x)/2}Fe^{(5-\delta)+}_{(1-x)/2}O_3. \quad (3)$$

He reported a disproportionation for $La_xSr_{1-x}FeO_{3-y}$ with $x \simeq 0.3$ below 200 K. This CD transition was abrupt and was accompanied by both a simultaneous metal-to-insulator transition and antiferromagnetic ordering. Matsuno *et al.* [7] also showed that the transition for $x = 1/3$ had the clearest temperature-dependent changes. A neutron diffraction study performed by Battle *et al.* [8] showed that two kinds of Fe ions with valence states Fe^{3+} and Fe^{5+} were found in a ratio of 2:1 below 200 K. In this CD state, a sequence of $Fe^{3+}(\uparrow)Fe^{3+}(\uparrow)Fe^{5+}(\uparrow)$ $Fe^{3+}(\downarrow)Fe^{3+}(\downarrow)Fe^{5+}(\downarrow)$ exists along the [111] direction of the pseudocubic perovskite unit cell. Previously, the detailed feature of the CD transition in $Sr_2LaFe_3O_{8+y}$ had been studied by using a Mössbauermeasurement, and first-order like transition from a high-temperature paramagnetic average-valence state in which all Fe cations are electronically equivalent to a low-temperature antiferromagnetic mixed-valence state was found [9]. The increase in the oxygen vacancy concentration was also reported th depress the transition temperature and to cause a degree of relaxational collapse in the magnetic hyperfine pattern. More recently, such a CD state was verified by transmission electron microscopy [10]. Park *et al.* found that when the R-site ion in $R_{1/3}Sr_{2/3}FeO_3$ was changed from La to Gd, the distortion of the FeO_6 octahedra increased with decreasing bond angle ∠Fe-O-Fe from 180° in an ideal cubic perovskite structure [11]. He suggested that such a distortion decreased the strength of the *p*-*d* hybridization interaction, hence reducing the stability of CD state.

Now, it will be of interest to observe the CD transition when the lanthanum content x is changed while the amount of the rare-earth ion-fixed species is kept constant. In this paper, will be presented results of XRD and Mössbauerspectroscopy for $La_xSr_{1-x}FeO_{3-y}$ with $x = 1/10$, $1/3$, and $1/2$ in order to see how the lanthanum content and the crystal structure influence the charge disproportionation transitions across their transition temperatures.

II. EXPERIMENT

The $La_xSr_{1-x}FeO_{3-y}$ polycrystalline samples ($x = 1/10$, $1/3$, and $1/2$) were prepared by using the conventional solid state sintering method starting with La_2O_3, Fe_2O_3, and SrO powders in appropriate proportions. In order to prevent any inaccuracy in the composition involved when using carbonate powder containing moisture, pure strontium-oxide powder was precisely weighed in a glove box filled with N_2 gas. A mixture of the compounds was intimately ground and fired at 900 °C for 9 hours for calcination. After regrinding, followed by press-molding into a pellet, thw samples were sintered at 1200 °C under atmosphere for 2 days and then slowly cooled down to room temperature for 4 days to attain maximum oxidation. In order to obtain a homogeneous material, we repeated this process twice.

X-ray diffraction (XRD) patterns of the samples were obtained with Cu Kα radiation. The patterns at room temperature were taken at a slow scanning speed of 0.5° advance in 2θ per min. to enhance the resolution. To determine the nominal Fe^{4+} content, we carried out chemical analyses by digestion in a standardized solution of Mohr salt in the presence of HCl and by titration with $K_2Cr_2O_7$ standard solution using the appropriate indicator [12]. A Mössbauerspectrometer of a conventional transmission-type was used in the constant acceleration mode. A ^{57}Co source in an Rh matrix with an activity of 15 mCi was used at room temperature.

III. RESULTS AND DISCUSSION

From the chemical analysis, the oxygen deficiencies, y, were found to be $0.17(x = 1/10)$, $0.04(x = 1/3)$, and $0.025(x = 1/2)$, showing a rapid decrease with increasing lanthanum content. Actually, Mizusaki *et al.* [13] reported that below 200 °C in an atmosphere of $P_{O_2} \geq 0.13$ atm, the oxygen vacancy y in $La_xSr_{1-x}FeO_{3-y}(0.4 < x < 1)$ was close to zreo. Stoichiometric formulas for the samples below and above the CD transition temperature deduced from the chemical analyses are summarized in the first row of the Table 2.

The XRD powder patterns of the compounds all show a single phase with no trace of impurity. Profile refinements were carried out by using the GSAS program package [14] in space group $R\bar{3}c$. For $x = 0.1$, $La_xSr_{1-x}FeO_{3-y}$is generally thought to be a normal cubic perovskite with a space group $Pm3m$ [15]. However,

Table 1. Structural parameters, bonding lengths, and bonding angles for $La_xSr_{1-x}FeO_{3-y}$at room temperature (SG: $R\bar{3}c$, hexagonal setting; x (O4): x position of oxygen atom; Occ (O4): occupation of oxygen sites).

		$x = 1/10$	$x = 1/3$	$x = 1/2$
a_H(Å)		5.4533	5.4927	5.5135
c(Å)		13.3667	13.4349	13.4255
V(Å^3)		344.25	351.03	353.44
x (O4)		0.509	0.519	0.535
Occ (O4)		0.941	0.987	0.992
U_{iso} (LA1/SR2)		0.005	0.006	0.008
U_{iso} (FE3)		0.006	0.003	0.008
U_{iso} (O4)		0.001	0.001	0.001
$_WR_P$		0.157	0.180	0.248
R_P		0.107	0.091	0.122
Bond Lengths (Å)	FE3 - O4 × 6	1.929(1)	1.943(9)	1.955(3)
	LA1/SR2 - O4 × 6	2.728(3)	2.745(7)	2.752(8)
	LA1/SR2 - O4 × 3	2.776(2)	2.851(1)	2.952(1)
	LA1/SR2 - O4 × 3	2.678(2)	2.641(1)	2.562(1)
Bond Angles (°)	∠ FE3 - O4 - FE3	177.1	173.8	168.6
	∠ O4 - FE3 - O4	180.00	180.00	180.00
	∠ O4 - FE3 - O4	90.01	90.14	90.51
	∠ O4 - FE3 - O4	89.99	89.86	89.49

to compare its bonding lengths and angles with those of other samples prepared, it was refined in the rhombohedral space group. In the process of refinements, we assumed that there were no orderings in either the La/Sr cations or the oxygen vacancies. Oxygen fractions were fixed to the values obtained from the chemical analyses. Finally, a profile function formed by a convolution of a pseudo-Voigt shape (CW profile #2 provided in the package) was used. The refinement results are listed in Table 1. The final observed and calculated room-temperature XRD profiles for $x = 1/3$ are illustrated in Fig. 1. Close examination of the difference curve indicated that a major error arises from improper selection of the profile function. However, for a comparison among samples of various compositions, the profile type was fixed to that which had given the best result for $x = 1/3$ sample in the course of refinements with no further attempt to use any other profile functions.

As x was changed from 1/10 through 1/3 to 1/2, the lattice constant a_H increased continuously. However, c increased and then decreased a little, eventually resulting in a gradual increase in the unit cell volume. The hexagonal lattice constants a_H and c can be converted to their rhombohedral analogues a_R and α_R [16]. Lanthanum substitution leads to an increase in a_R from 5.4557 Å(x = 1/10) through 5.4874 Å(x = 1/3) to 5.4918 Å(x = 1/2) and an increase in the edge angle α_R from 59.97° (x = 1/10) through 60.07° (x = 1/3) to 60.26° (x = 1/2), namely an increase in the rhombohedral lattice distortion. More detailed aspects of the distortion in a FeO_6 octahedron can be seen by examining both the Fe-O bond length and the bond angles ∠O-Fe-O and ∠Fe-O-Fe. While the Fe-O bond lengths increased with increasing lanthanum content, ∠O-Fe-O bond angles remained almost unchanged, although a very slight increase in rhombohedral distortion was obvious. This means that as the lanthanum content was increased, elongation of the Fe-O distances induces expansion of each FeO_6 octahedron while maintaining its shape with no distortion. On the other hand, the ∠Fe-O-Fe bond angle continuously decreases from 177.1° to 168.6°. This indicates that as x was increased, the degree of zigzag tilting between any two octahedra increased with no distortions in

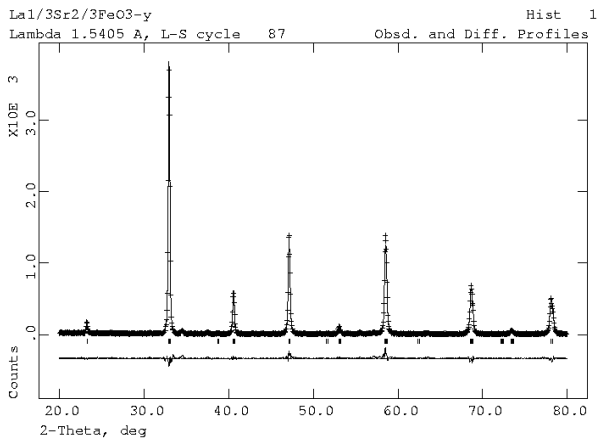

Fig. 1. Observed ($\cdots$), calculated (−), and difference curves in the XRD profile for $La_xSr_{1-x}FeO_{3-y}$($x = 1/3$).

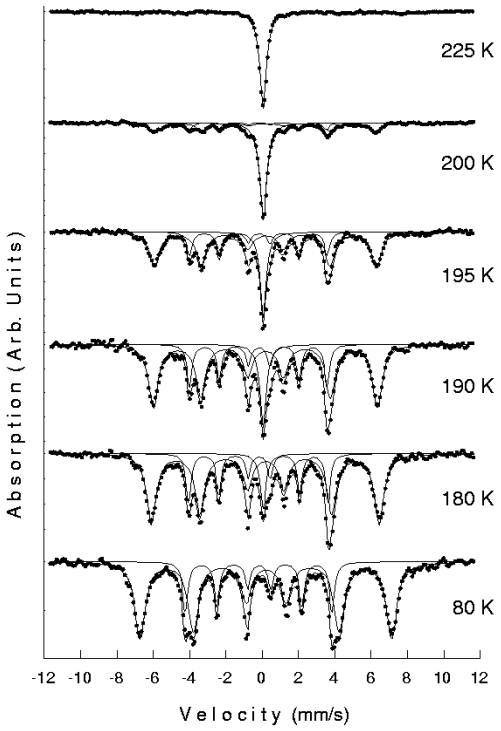

Fig. 2. Mössbauerspectra for $La_xSr_{1-x}FeO_{3-y}(x = 1/3)$ at various temperatures

the FeO_6 octahedra. La or Sr ions behave just like rigid spheres. For $x = 1/10$, the ∠O-Fe-O bond angles with six neighboring oxygen ions were 90° and 180° within experimental error, which means that this compound is close to a perfect cubic perovskite. The magnitude of the distortion in a perovskite can be discussed in terms of a tolerance factor t defined by

$$t = \frac{d_{\mathrm{La/Sr-O}}}{\sqrt{2}\, d_{\mathrm{Fe-O}}}. \quad (4)$$

If cations and oxygen are located such that $t = 1$, presumably they will form an ideal cubic perovskite. For those with t slightly less than 1, the FeO_6 octahedra are rotated about the (111) axis, giving rise to a rhombohedral unit cell. For smaller t, the octahedra tilt about the (110) and the (001) directions, resulting in the orthorhombic $GdFeO_3$ structure. For even smaller t, other non-perovskite structures become favored. If the values of bond lengths listed in Table 1 are used to determine t for the compounds, the calculated tolerance factors are 1.000 ($x = 1/10$), 0.999 ($x = 1/3$), and 0.996 ($x = 1/2$). There is a well-defined boundary at $t = 0.985$ above which rhombohedral structures are formed and below which the atoms form an orthorhombic structure [17]. It can be concluded from the magnitude of the tolerance factors that for $x = 1/10$, this compound is close to a perfect cubic perovskite whereas for both $x = 1/3$ and 1/2, these are perovskites with very slight rhombohedral

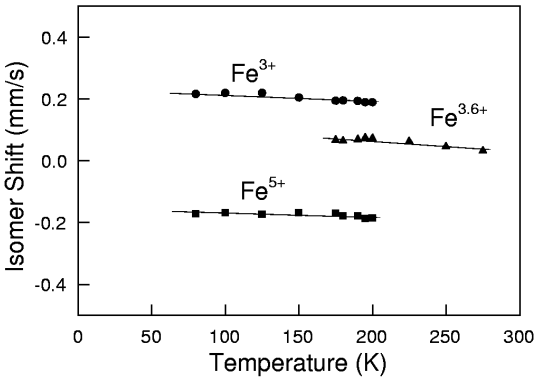

Fig. 3. Variation of the isomer shift δ for $La_xSr_{1-x}FeO_{3-y}(x = 1/3)$ with temperature

distortion. This is an expected result in view of the fact that for $x = 1/10$, the ∠O-Fe-O bond angles were all 90° within experimental error whereas for both $x = 1/3$ and 1/2, there were slight rhombohedral distortions.

Park *et al.* [11] showed that as the angle ∠Fe-O-Fe deviated from 180°, hybridization t_{p-d} decreased and the CD transition became not obvious. Since the above-mentioned structural distortion will reduce the hybridization t_{p-d} between Fe($3d$) and O($2p$), apparent Mössbauerspectroscopic differences across the CD transitions are expected among the compounds. Figure 2 depicts the Mössbauerspectra for $La_xSr_{1-x}FeO_{3-y}(x = 1/3)$ taken at various temperatures. At 80 K, the spectrum is comprised of two superimposed magnetic hyperfine patterns with magnetic hyperfine fields of 43.2 and 25.1 T and isomer shifts of 0.25 and -0.17 mm/s, respectively. The outer component of the spectrum was ascribed to Fe^{3+} ions in the octahedral sites and the inner one to Fe^{5+} ions in the octahedral sites. This is the mixed-valence state produced by the CD into species approximating to Fe^{3+} and Fe^{5+}. The experimental area ratio at 175 K was 74:26. Chemical analysis indicates that 1.3 % of the oxygen sites are vacant, and the expected Fe^{3+}: Fe^{5+} area ratio is 71:29 under the assumption that they have the same recoil free fraction. Considerable collapse of the hyperfine pattern took place much below the expected ordering temperature. In the temperature range between 175 K and 200 K, the high-temperature paramagnetic average-valence state and the low-temperature antiferromagnetic mixed-valence state coexisted. As the temperature rose, the central paramagnetic line grows, while the magnetic sextets continuously diminished.

The variation of the isomer shifts for $La_xSr_{1-x}FeO_{3-y}(x = 1/3)$ with temperature is shown in Fig. 3. In the temperature range from 175 K to 200 K, the isomer-shift values for two low-temperature sextets are $0.19(Fe^{3+})$ and $-0.18(Fe^{5+})$ mm/s and that for a high-temperature single line is 0.07 mm/s. However, closer examination reveals that the valence state of the high temperature phase is about +3.6 rather than +4,

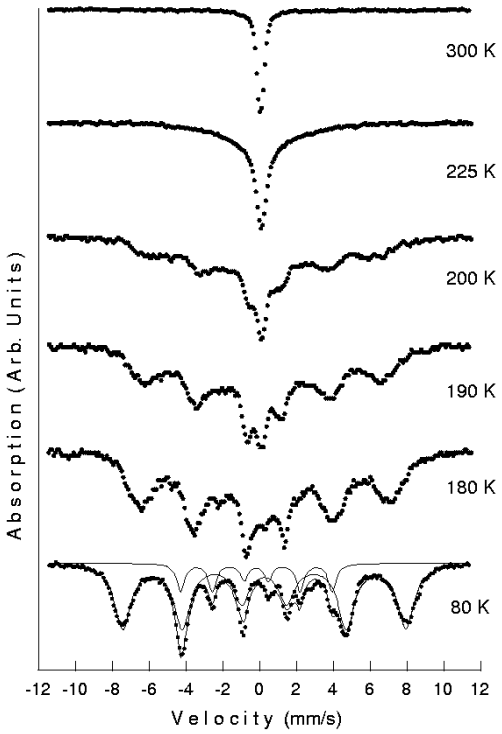

Fig. 4. Mössbauerspectra for $La_xSr_{1-x}FeO_{3-y}(x = 1/2)$ at various temperatures. No attempt was made to fit the spectra above 175 K due to heavy overlap.

which can be given by the following weight averaging

$$Fe^{3.6+} \rightleftharpoons 0.71Fe^{3+} + 0.29Fe^{5+}, \quad (5)$$

assuming a linear relationship between the isomer shift and the valence of the iron ion.

There are no quadrupole splittings within experimental error. This is consistent with the fact that the electronic configurations of both $Fe^{3+}(t_{2g}^3e_g^2)$ and $Fe^{5+}(t_{2g}^3)$ are highly symmetric. It is clear from the Mössbauerspectra that the width of the absorption line for Fe^{3+} is much broader than that for Fe^{5+}. This originates from the fact that a Fe^{3+} has three Fe^{3+} and three Fe^{5+} neighbors while a Fe^{5+} has six Fe^{3+} as neighbors, indicating that the site symmetry for Fe^{5+} is higher than that for Fe^{3+}. At elevated temperatures above 200 K, only the paramagnetic singlet from $Fe^{3.6+}$ can be seen. Although the content of Fe^{4+} was definitely determined from the chemical analysis, it was not possible to single out the absorption line for Fe^{4+} in the spectra. This can be explained by an itinerant σ^* band derived from the e_g electron in high-spin $Fe^{4+}(t_{2g}^3e_g^1)$. At this time, an electron can hop from one Fe to another, generating both an intermediate valence state and metallic conductivity. When such a fast hopping of electrons exists, fluctuations of hyperfine parameters for the ^{57}Fe nucleus will take place, resulting in a relaxation effect as can be observed in the singlet spectrum above 200 K. If Fe^{4+} ions are in high-spin states and their $3d$ electrons are localized, Jahn-Teller distortion should take place. However, they avoid such a distortion through fast hopping, resulting in a vanishing electric quadrupole splitting.

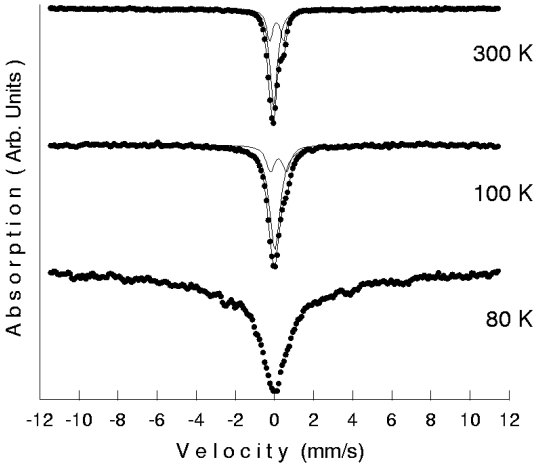

Fig. 5. Mössbauerspectra for $La_xSr_{1-x}FeO_{3-y}(x = 1/10)$ at various temperatures

Figure 4 gives typical Mössbauerspectra for $x = 1/2$ for various temperatures. The hyperfine fields at 80 K were 46.8 and 25.6 T corresponding to charge disproportionated Fe^{3+} and Fe^{5+} states, respectively. The experimental area ratio at 80 K was 80:20. The same kind of CD transition as in $x = 1/3$ was also observed in the temperature range 175 $\sim$ 225 K. However, the spectra were collapsed by heavy broadening or severe superposition, resulting in an unclear transition. This is in contrast to the case of $x = 1/3$, in which the separation between Fe^{3+} and Fe^{5+} was manifestly seen until the CD transition was completed. From the values of the isomer shifts, 0.27 and -0.15 mm/s at 80 K, the two spectral components below the CD transition can be assigned to Fe^{3+} and Fe^{5+}. The isomer shift at 225 K, which is just above the CD transition temperature, is 0.07 mm/s, and this corresponds to the isomer shift value of the intermediate valence state between Fe^{3+} and Fe^{5+}.

Figure 5 shows the Mössbauerspectra of $La_xSr_{1-x}FeO_{3-y}(x = 1/10)$ taken at various temperatures. The spectrum at 80 K is very broad and poorly resolved, indicating that it is very close to the magnetic transition temperature. These spectra closely resemble those of oxygen-deficient $SrFeO_{2.86}$ prepared under atmosphere, whose Néeltemperature was 80 K [18]. Gibb proposed a model in which there were three doublets for the paramagnetic Mössbauerspectra of his oxygen-deficient $SrFeO_{2.844}$ [19], which showed similar properties as the present sample. However, the velocity ranges of the spectra obtained in the present study were so wide (-12 mm/s $\sim$ 12 mm/s) that they could not offer enough detailed resolution. The spectra above 100 K consist of a quadrupole doublet and a singlet. At 300 K, the absorptions at 0.46 and -0.24 mm/s can be attributed to a component of the symmetrical

Table 2. Results of chemical analysis and Mössbauerparameters at 80 K (100 K for $x = 1/10$) and 300 K for $La_xSr_{1-x}FeO_{3-y}$. (Subscript S: singlet, D: doublet, 1 or 2: hyperfine sextets; units for the isomer shift δ and the quadrupole splitting Δ are mm/s, and that for hyperfine field H is Tesla).

	$x = 1/10$	$x = 1/3$	$x = 1/2$
Chemical formulas ($T > T_{CD}$)	$La_{1/10}Sr_{9/10}Fe^{4+}_{0.775}Fe^{3+}_{0.225}O_{2.83}$	$La_{1/3}Sr_{2/3}Fe^{4+}_{0.6}Fe^{3+}_{0.4}O_{2.96}$	$La_{1/2}Sr_{1/2}Fe^{4+}_{0.45}Fe^{3+}_{0.55}O_{2.975}$
($T < T_{CD}$)		$La_{1/3}Sr_{2/3}Fe^{5+}_{0.3}Fe^{3+}_{0.7}O_{2.96}$	$La_{1/2}Sr_{1/2}Fe^{5+}_{0.22}Fe^{3+}_{0.78}O_{2.975}$
80 K	$\Delta_D = 0.80$ $\delta_D = 0.20$ $\delta_S = 0.021$ A_D:A_S = 27:73	$H_1 = 43.2$ $\delta_1 = 0.25$ $H_2 = 25.1$ $\delta_2 = -0.17$ A_1:A_2 = 77:23	$H_1 = 46.8$ $\delta_1 = 0.27$ $H_2 = 25.6$ $\delta_2 = -0.15$ A_1:A_2 = 83:17
300 K	$\Delta_D = 0.70$ $\delta_D = 0.11$ $\delta_S = -0.04$ A_D:A_S = 34:66	$\delta_S = 0.02$	$\delta_S = 0.07$

quadrupole doublet and that at -0.04 mm/s to the other singlet. An investigation of the isomer-shift of the doublet leads to an average-valence ($Fe^{3.5+}$) due to hopping to this component. The observed quadrupole splitting probably results from particular ordering of oxygen vacancies [20]. The most intense singlet is assigned to the delocalized Fe^{4+} state. The singlet : doublet area ratio was about 79 : 21, which is close to the ratio 83 : 17 predicted by the stoichiometric formula deduced from chemical analysis. Also, for the present case of $x = 1/10$, our study confirms the hypothesis of Takeda *et al.*, *i.e.*, the existence of the so-called average valence state produced by short-range hopping. Bocquet *et al.* [21] had already found that the ground state of $SrFeO_3$ was heavily mixed, producing the large covalency. The charge transfer energy was negative, meaning that charge could be easily transferred via Fe-O bonds from the O $2p$ bands to the metal d orbitals. The abovementioned short-range hopping and the metallic conductivity are interpreted as stemming from this small value of the charge transfer energy.

In the present study, when x was increased from 1/3 to 1/2, the CD transition became blurred with its transition temperature effectively unchanged. Park *et al.* [11] reported that as the distortion of the FeO_6 octahedra was increased to decrease the bond angle ($\angle$Fe-O-Fe) from 180°, hybridization between the oxygen $2p$ σ and the Fe $3d$ e_g state was weakened: accordingly, the electron transfer interaction decreased, which made the CD state unstable and the CD transition unclear. Unfortunately, corresponding data for bond angles and bond lengths are not available. The magnitude of the tolerance factor for the $Pr_{1/3}Sr_{2/3}FeO_3$ ($t = 0.996$) of Park *et al.* is similar to that for the present $La_xSr_{1-x}FeO_{3-y}(x = 1/2)$. Also, the corresponding transition of $Pr_{1/3}Sr_{2/3}FeO_3$ shows a somewhat more collapsed feature than $La_{1/3}Sr_{2/3}FeO_3$ does. This kind of collapsed feature is also observed in the Mössbauerspectra of $La_xSr_{1-x}FeO_{3-y}(x = 1/2)$. In fact, in the cases of $Pr_{1/3}Sr_{2/3}FeO_3$ and $Nd_{1/3}Sr_{2/3}FeO_3$, the CD transition became blurred with its transition temperature shifted to lower temperature in comparison with the case of $La_{1/3}Sr_{2/3}FeO_3$. On the contrary, Lacorre *et al.* [17] announced for a series of $RNiO_3$ compounds that such a transition temperature was observed to decrease as the tolerance factor increased. Although the direct comparison between the two cases is not adequate, these two contradicting tendencies lead us to conclude that such tiny decreases in the bond angle ($\angle$Fe-O-Fe) from 180° do not affect the electron hopping mechanism so much. Rather, controlling the Fe-O bond lengths seems to be a more effective way to vary the electronic properties of these materials. This can be seen affirmatively in the present case for $x = 1/10$. The magnetic coupling via the Fe-O-Fe pathway is predicted to be strong G-type antiferromagnetic [22]. However, in spite of the superexchange angle being exactly 180°, its magnetic transition temperature is very low. Excessive contractions in bond lengths change the hybridization or possibly the electron transfer energy, which again enhance the electron conduction. This depresses the electronic delocalization temperature, and no CD transition was observed for $x = 1/2$ and 1/3. This compound is anticipated to show metallic behavior down to very low temperature with no CD transition. The other possible origin affecting the electron transfer interaction is the carrier doping level x. However, it was already known that the electronic transition could be made unclear, or such a transition could even be disappeared only by controlling the tolerance factor without varying the doping level [11]. Thus the effects of the doping level will not be discussed any further.

In conclusion, the crystallographic and the magnetic properties of polycrystalline $La_xSr_{1-x}FeO_{3-y}(x = 1/10$, 1/3, and 1/2) were studied. From the chemical analysis, oxygen deficiencies, y, were found to decrease rapidly with increasing lanthanum content. As the lanthanum content x was increased, both the rhombohrdral lattice constant a_R and the edge angle α_R increasd, resulting in a slight increase in the tolerance factor t. From the temperature variations of the Mössbauerspectra, the CD transition for $x = 1/3$ was found to be the most outstanding among the samples prepared. As the lanthanum

content x was increased to 1/2, the CD transition was somehow blurred by the weakened $p-d$ hybridization due to a decrease in bond angle ($\angle$Fe-O-Fe) from 180°. For the case of $x = 1/10$, in which a strong magnetic interaction was expected, the electron delocalization took place at a very low temperature; finally, it was paramagnetic in the temperature region examined dueto a reduction of the electron transfer energy caused by the contractions in bond lengths. All the characteristics of the sample for $x = 1/10$ seem to be closer to those of $SrFeO_3$ than to those of $La_{1/3}Sr_{2/3}FeO_3$.

ACKNOWLEDGMENTS

This work was supported by grant No. R05-2001-000-00128-0 from the Basic Research Program of the Korea Science & Engineering Foundation.

REFERENCES

[1] S. W. Han, J. D. Lee, K. H. Kim, H. Song, W. J. Kim, S. J. Kwon H. G. Lee, C. Hwang, J. I. Jeong and J. S. Kang, J. Korean Phys. Soc. **40**, 501 (2002).
[2] A. Chainani, M. Mathew and D. D. Sarma, Phys. Rev. B **48**, 14818 (1993).
[3] M. Takano, N. Nakanishi, Y. Takeda, S. Naka and T. Takeda, Mater. Res. Bull. **12** 923 (1977).
[4] T. Takeda, Y. Yamaguchi and H. Watanabe, J. Phys. Soc. Jpn. **33**, 967 (1995).
[5] U. Shimony and J. M. Knudsen, Phys. Rev. **144**, 361 (1966).
[6] M. Takano, J. Kawachi, N. Nakanishi and Y. Takeda, J. Solid State Chem. **39**, 75 (1981).
[7] J. Matsuno, T. Mizokawa, A. Fujimori, K. Mamiya, Y. Takeda, S. Kawasaki and M. Takano, Phys. Rev. B **60**, 4605 (1999).
[8] P. D. Battle, T. C. Gibb and P. Lightfoot, J. Solid State Chem. **84**, 271 (1990).
[9] P. D. Battle, T. C. Gibb and S. Nixon, J. Solid State Chem. **77**, 124 (1988).
[10] J. Q. Li, Y. Matsui, S. K. Park and Y. Tokura, Phys. Rev. Lett. **79**, 297 (1997).
[11] S. K. Park, T. Ishikawa, Y. Tokura, J. Q. Li and Y. Matsui, Phys. Rev. B **60**, 10788 (1999).
[12] D. T. Sawyer, W. R. Heineman and J. M. Beebe, *Chemistry Experiments for Instrumental Methods* (Wiley, New York, 1984).
[13] J. Mizusaki, M. Yoshihiro, S. Yamauchi and K. Fukei, J. Solid State Chem. **58**, 258 (1985).
[14] A. C. Larson and R. B. von Dreele, *General Structure Analysys System*, Report No. LAUR-86-748 (Los Alamos National Laboratory, Los Alamos, 1990).
[15] S. E. Dann, D. B. Currie, M. T. Weller, M. F. Thomas and A. D. Al-Rawwas, J. Solid State Chem. **109**, 134 (1994).
[16] B. D. Cullity, *Elements of X-Ray Diffraction*, 2nd ed. (Addison Wesley, Massachusetts, 1978).
[17] P. Lacorre, J. B Torrance, J. Pannetier, A. I. Nazzal, P. W. Wang and T. C. Huang, J. Solid State Chem. **91**, 225 (1991).
[18] P. K. Gallagher, J. B. MacChesney and D. N. E. Buchanan, J. Chem. Phys. **41**, 2429 (1964).
[19] T. C. Gibb, J. Chem. Soc. Dalton Trans., 1455 (1985).
[20] L. Fournes, Y. Potin, J. C. Grenier, G. Demazeau and M. Pouchard, Solid State Commun. **62**, 239 (1987).
[21] A. E. Bocquet, A. Fujimori, T. Mizokawa, T. Saihto, H. Namatame, S. Suga, N. Kimizuka, Y. Takeda and M. Takano, Phys. Rev. B **45**, 1561 (1992).
[22] J. B. Goodenough, *Magnetism and the Chemical Bond* (Wiley, New York, 1971).